

2D AND 3D MODELLING OF OFFSHORE SANDBANK DYNAMICS

STEPHEN CLEE⁽¹⁾, PROFESSOR SHUNQI PAN⁽²⁾

⁽¹⁾ SCHOOL OF ENGINEERING, CARDIFF UNIVERSITY, CF24 3AA, UNITED KINGDOM
E-MAIL: CLEESA@CARDIFF.AC.UK

⁽²⁾ SCHOOL OF ENGINEERING, CARDIFF UNIVERSITY, CF24 3AA, UNITED KINGDOM
E-MAIL: PANS2@CARDIFF.AC.UK

ABSTRACT

The coastal zone is an important resource both socially and economically. Globally, coastal zones are under increasing threat from the effects of climate change, erosion and flooding. Understanding the mechanisms of coastal processes is key to the long term management and protection of the coastal zone and its resources. Sandbanks are large sedimentary bodies found on coastal shelves worldwide that protect nearby coastlines from the effects of erosion. This research aims to model the hydrodynamics and morphodynamics of the sandbanks in the southern bight of the North Sea, UK. The main objective is to determine the impact of the vertical velocity component on the recirculation of the flow and on the suspended and bedload sediment transport rates and how this affects the long term behaviour of a sandbank under normal and storm conditions. The study site for this research is the southern bight of the North Sea covering an area of roughly 85600km². This research uses the TELEMAC suite comprising of TELEMAC2D for 2D hydrodynamics, TELEMAC3D for 3D hydrodynamics and SISYPHE for 2D and 3D morphodynamics. This paper presents the details of model setup, calibration process and both 2D and 3D hydrodynamic results focussed on an area of sandbanks in the domain.

Keywords: Offshore sandbanks, TELEMAC, Hydrodynamics, North Sea

1 INTRODUCTION

It is estimated by the United Nations that by 2020 nearly 75% of the world's population will live in or near to the coastal zone. Coastal environments offer a variety of important economic, residential and recreational functions, all of which depend on its physical characteristics. With increased pressure on coastal regions due to the effects of climate change and sea level rise there is great scope to expand current coastal management schemes. Improving our understanding of the complex governing processes is critical in order to protect this vital resource for future generations (Chadwick et al. 2012).

Sandbanks are large offshore sedimentary bodies which are found on most coastal shelves around the world. Most shallow tidal seas where currents exceed 0.5ms⁻¹ and also have an abundant supply of sediment will have sandbanks present. (Dyer & Huntley 1999) define sandbanks as having a length up to 80km, an average width of typically 13km, height of tens of metres and spacing proportional to the width. (Stride 1982) divides sandbanks into two classes; actively maintained banks which are characterised by shallow crests, asymmetrical crest and near surface currents above 0.5ms⁻¹, and moribund banks which are characterised by rounded crests, shallower slopes and near surface currents below 0.5ms⁻¹.

Offshore sandbanks affect navigation and offshore structures but also provide protection to the adjacent stretches of coastlines by dissipating incoming wave energy. Sandbanks are an important habitat and feeding ground for a wide variety of marine organism such as worms, crustaceans, molluscs, echinoderms, shrimps, crabs, fish and eels (JNCC 2017). Understanding the development and evolution of offshore sandbanks presents a challenge due to the complex interactions between tidal currents, waves and sediment. This is significant when taking the effects of climate change and sea level rise into account.

Geometric characteristics of the largest sandbanks are not just dependent on the sediment properties and tidal condition but also the rotational direction of the velocity vectors (Besio et al. 2005). In the northern hemisphere, the Coriolis force creates vorticity which enhances growth in an anticlockwise direction relative to the flow (Garel 2010).

Artificially increasing the height of offshore and nearshore sandbanks has been considered as strategy to counter the effects of sea level rise on coastal erosion and flooding. However, the viability of this strategy is dependent on the local hydrodynamic conditions. Areas where the tidal conditions cause erosion of the natural sediment will also cause any artificially added sediment to be washed away. Also the benefits of artificially increasing the height of a sandbank are vastly reduced when considering offshore sandbanks compared to nearshore sandbanks (Stansby et al. 2006).

Theoretical aspects of sandbank growth have been investigated in a number of studies. These take into consideration the effects of hydrodynamics of the flow due to sandbank presence, sediment transport patterns around the sandbanks and the effects of growth on the hydrodynamics. However, they neglect to determine the effects of all these factors simultaneously. Computer models have been developed that predict the long term evolution of offshore sandbanks but have largely ignored the effects of waves and wave current interactions (Pan et al. 2007).

Sediment transport pathways in the wider North Sea region are well defined but there is more uncertainty about the localised sediment transport in the troughs between sandbanks. Observations suggest that currents flowing north are dominant over currents flowing to the south due to steeper slopes on the western flanks of the sandbanks (Caston & Stride 1970). (Brooks 2010) concluded that the tides in the region are predominately semi diurnal, entering from the south during the flood period and the north during the ebb period. Short term sediment transport patterns show convergence on the crests on sandbanks but it is difficult to predict long term sediment transport based on short term hydrodynamic measurements (Garel 2010). (Jacoub et al. 2007) suggests a need for long term sediment transport modelling (of the order of 20-30 years) to accurately assess the impacts of coastal erosion and sandbank evolution.

The research aims to evaluate the differences between 2D and 3D modelling of the hydrodynamics and morphodynamics, looking specifically at the sandbanks in the North Sea region. It aims to determine the differences between 2D and 3D hydrodynamic models and the resultant impact this has upon sediment transport and long term evolution of sandbanks in the study area.

2 MODEL SETUP

The software used in this study is TELEMAC2D and TELEMAC3D (HR Wallingford 2016), an integrated suite of solvers for free surface flows in 2D and 3D respectively. The study site for this research is the southern bight of the North Sea covering a region from 0.6°E to 6°W and 50.8°N to 54°N. An unstructured triangular mesh was created consisting of three different grids. First, a coarse grid to cover the large expanses of open sea. Second, an intermediate grid to cover areas close to the coastlines. Finally, a fine grid to cover an area of the Indefatigable banks which are located approximately 50km off the Norfolk coastline. Experimentation with different mesh sizes in (Kuang & Stansby 2006) concluded that fine and intermediate meshes with a varying cell size of 360-1530m have more comparable results for sediment transport than coarser meshes. This is due to the failure of coarse meshes to resolve recirculating flows around sandbanks. As such, it was concluded to use a grid size of 2500m for the coarse grid, 500m for the intermediate grid and 100m for the fine grid. This was done to provide an acceptable balance between computational effort and overall model accuracy. The final mesh covers an area of 85572.022km² and consists of 450344 nodes and 895657 elements.

Bathymetry data was obtained for the region from the British Oceanographic Data Centre (BODC) at intervals of 30 arc seconds. This was then mapped onto the mesh using the inverse distance interpolation method, shown in Figure 1.

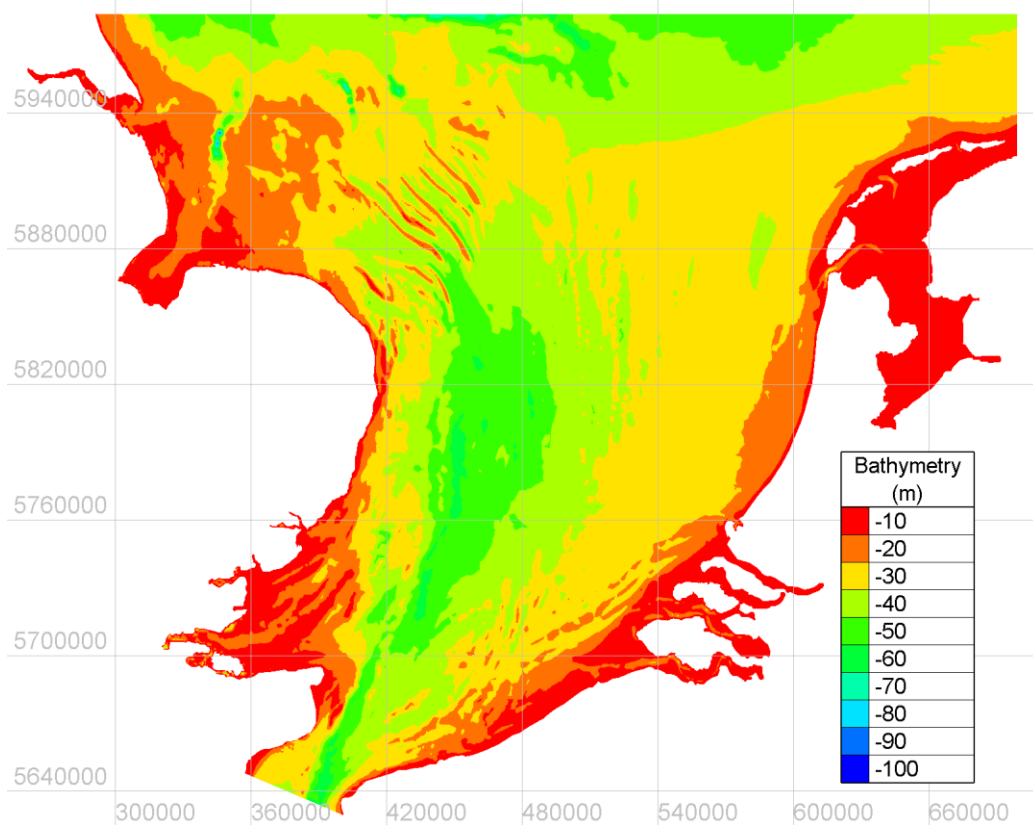


Figure 1. Computational domain with mapped bathymetry

The model has four tidal boundaries; one in the north, one in the south, one representing the Thames estuary and the final boundary representing the Humber estuary. Tidal conditions were prescribed on the boundaries using the TPXO database from the Oregon State University (OSU) (Oregon State University 2010). The TPXO database provides tidal amplitudes and phases for 13 harmonic constituents.

3 2D MODEL – CALIBRATION AND VALIDATION

The model was calibrated to determine the values of four input parameters. Three parameters relate to the adjustment of the tidal boundary conditions: namely coefficient to calibrate sea level (CSL), coefficient to calibrate tidal range (CTR) and coefficient to calibrate tidal velocity (CTV). The fourth parameter for calibration relates to the friction coefficient. The coefficients are used to calculate the modified free surface level and tidal velocity as shown in equation 1.

$$\begin{aligned}
 h &= CTR \sum_i h_i - b + CSL \\
 u &= CTV \sum_i u_i \\
 v &= CTV \sum_i v_i
 \end{aligned}
 \tag{1}$$

Where;

- h_i is the water depth for harmonic constituent i
- u_i and v_i are the velocity components for harmonic constituent i
- b is the bed level elevation
- CSL, CTR and CTV are the values of the corresponding coefficients

Tidal elevation data was obtained for a two year period between January 1st 2016 and December 31st 2017 at 16 measurement stations across the domain shown in Table 1. Data was sourced from the British Oceanographic Data Centre (BODC) for stations 1-6, the Reseaux de reference des observations maregraphiques (REFMAR) for stations 7-8 and the North West Shelf Operational Oceanographic System (NOOS) for stations 9-16. Observation data was at 15 minute intervals for stations 1-6 and at 10 minute intervals for stations 9-16. The data sourced from the BODC and REFMAR is referenced to Chart Datum (CD) whereas the data sourced from the NOOS and the calculated outputs of the model are referenced to Ordnance Datum Newlyn (ODN). In order to convert between the two, the difference between the datums represented in Table 1 is added to the observation data.

Table 1. Tidal gauge station information.

Name	Number	Northing (m)	Easting (m)	CD to ODN (m)
Immingham	1	318419.406	5869120.000	-3.90
Cromer	2	386800.000	5867000.000	-2.75
Lowestoft	3	418000.000	5814268.500	-1.50
Harwich	4	385017.625	5753947.000	-2.02
Sheerness	5	342057.188	5700600.000	-2.90
Dover	6	383011.344	5663415.500	-3.67
Calais	7	454906.563	5657702.000	-3.99
Dunkerque	8	419043.813	5649670.500	-3.14
Westhinder	9	461035.000	5693345.000	0.00
Ostend	10	490030.156	5679014.500	0.00
Hoek van Holland	11	574928.938	5759094.500	0.00
Europlatform	12	519222.000	5761075.000	0.00
Ijmuiden	13	602897.938	5814126.000	0.00
K13a	14	630298.183	5943047.772	0.00
J61	15	496050.080	5963496.747	0.00
L91	16	514689.114	5896766.757	0.00

Velocity data was obtained from Admiralty Chart 2182A which covers the southern bight of the North Sea. The chart displays tidal currents at 20 points, 9 of which are inside the model domain. At each point the current is given at hourly intervals for times 6 hours before and 6 hours after the high water level at Dover. The locations of the 16 tidal gauge stations (numbered) and the 9 velocity points (lettered) are shown in Figure 2.

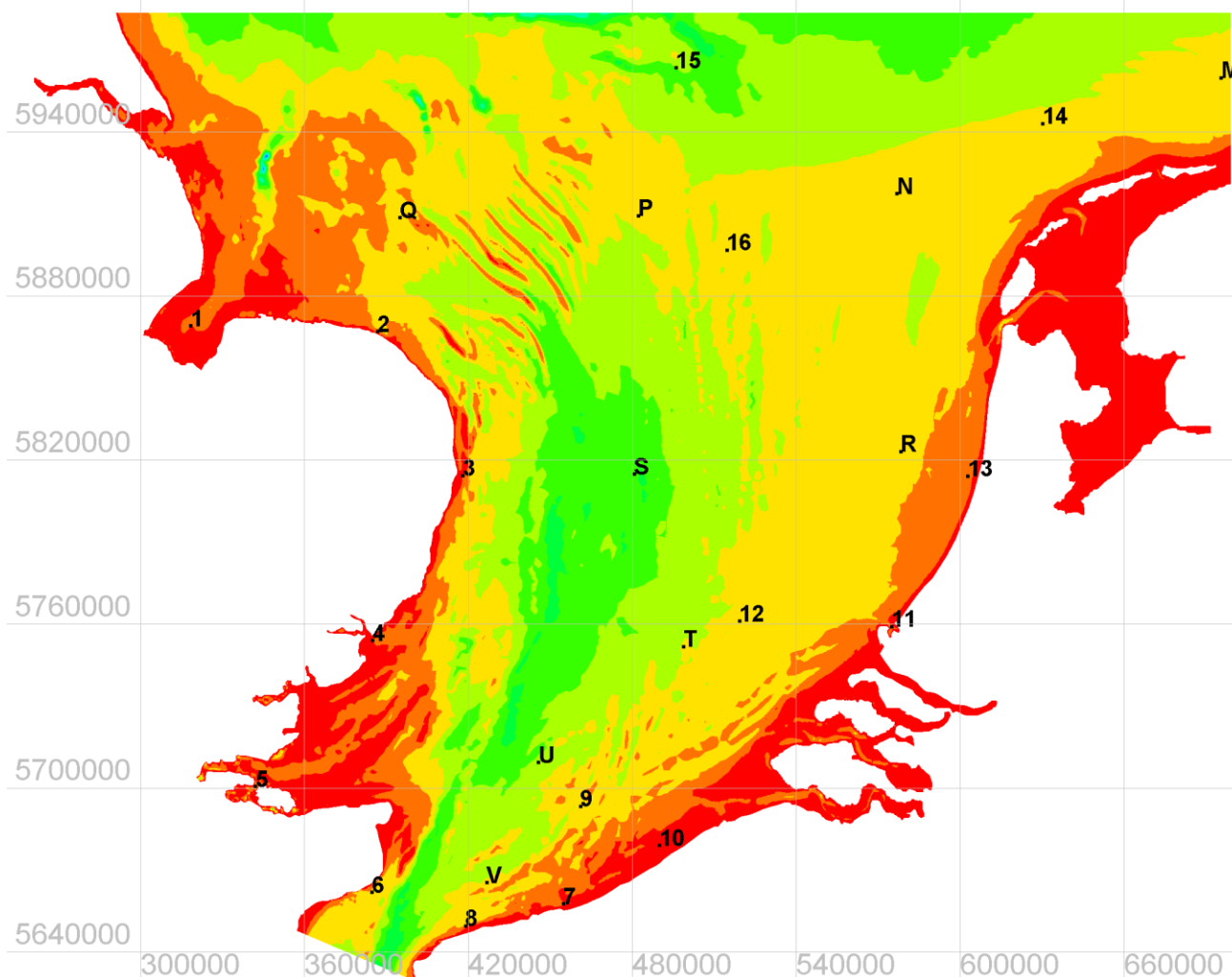


Figure 2. Location of calibration stations for free surface (1-16) and velocity (M-V).

In order to determine accurate values for each of the parameters, the model was calibrated against the observation data. Each case was set up to run for a duration of 15 days in order to cover at least one spring and one neap tidal cycle. The first case was run using the default values assigned to each coefficient. In order to evaluate the error and differences between the observed data and the calculated data for the free surface level, the root mean square error (RMSE) was calculated using equation 2.

$$RMSE = \frac{\sum_{t=1}^n (z_{obs} - z_{calc})^2}{n} \quad [2]$$

Where;

z_{obs} = Free surface elevation observed at timestep t (m)

z_{calc} = Free surface elevation calculated at timestep t (m)

n = number of timesteps

An average RMSE value was then calculated across all 16 stations. The value of one parameter was then modified and the average RMSE value for the new case compared with the current best case. This process was repeated until changing the value of a parameter no longer improved the average RMSE. At this point the coefficient was considered to be optimised and the method was repeated for the remaining parameters. The optimised values for each of the coefficients is shown in Table 2. The time series of the free surface elevation and velocity at several points throughout the domain is shown in Figures 3-7. When analysing the cases for the calibration coefficient for tidal velocity it was noted that changing the coefficient below 0.90 showed negligible improvement of the RMSE when comparing the observation and calculation data for the free surface elevation. However there was a noticeable difference when calculating the RMSE for the velocity data (shown in Table 3). It was calculated that the optimal value of CTV occurred for case V090. These results does carry a degree of uncertainty due to the limited availability of time series velocity data.

Table 2. RMSE values for free surface calibration.

Case	CSL	CTR	CTV	Friction Coefficient	Average RMSE (m)
Baseline	0.00	1.00	1.00	60	0.264
S007	0.07	1.00	1.00	60	0.256
T113	0.07	1.13	1.00	60	0.242
V090	0.07	1.13	0.90	60	0.240
F65	0.07	1.13	0.90	65	0.232

Table 3. RMSE values for velocity calibration

Case	CSL	CTR	CTV	Friction Coefficient	Average RMSE (ms ⁻¹)
V090	0.07	1.13	0.90	60	0.0095
V080	0.07	1.13	0.80	60	0.0097
V070	0.07	1.13	0.70	60	0.0100
V075	0.07	1.13	0.75	60	0.0103
V085	0.07	1.13	0.85	60	0.0107

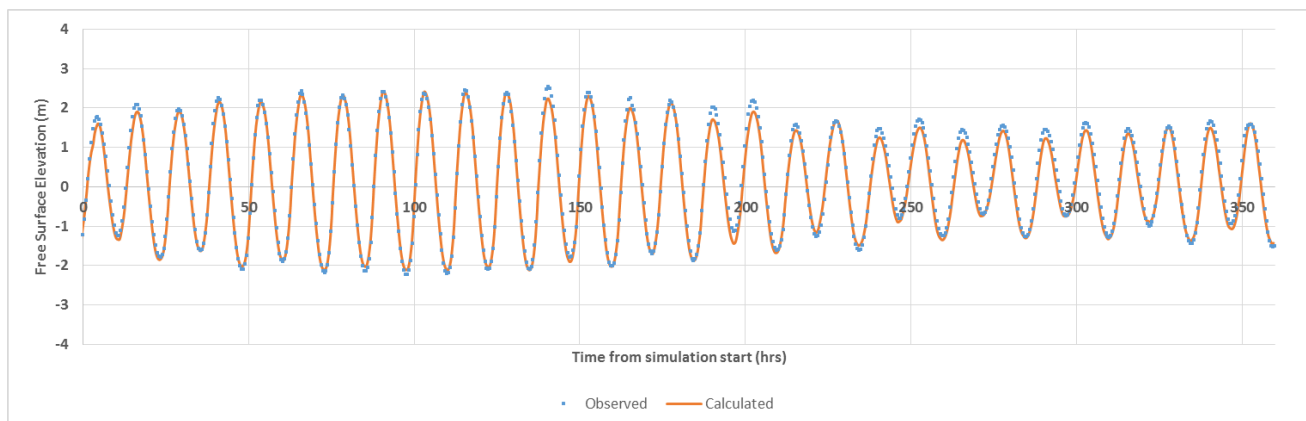


Figure 3. Observed against calculated free surface elevations at Cromer (station 2)

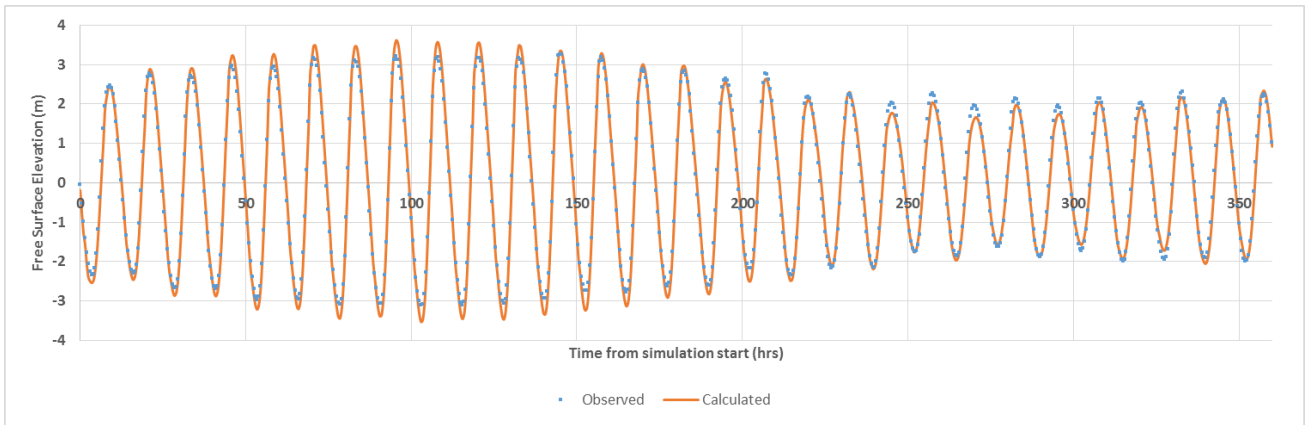


Figure 4. Observed against calculated free surface elevations at Dover (station 6)

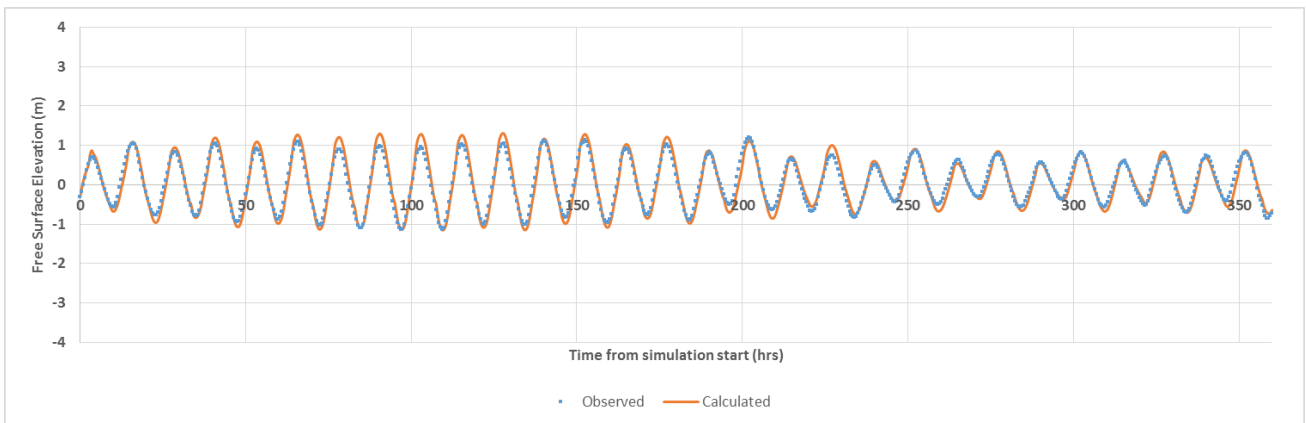


Figure 5. Observed against calculated free surface elevations at J61 (station 16)

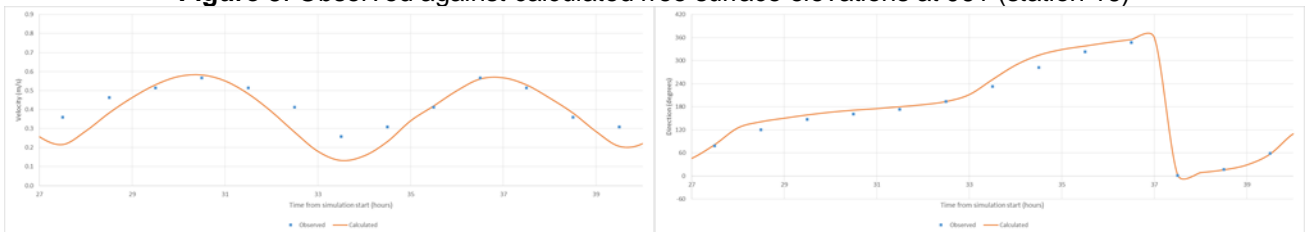


Figure 6. Observed against calculated velocity magnitude and direction at point P.

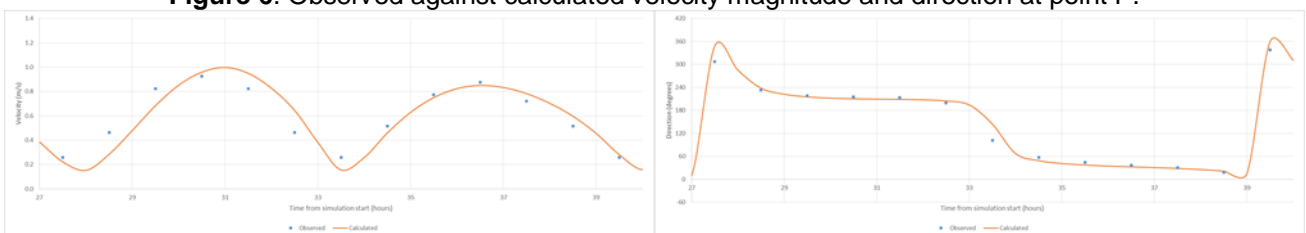


Figure 7. Observed against calculated velocity magnitude and direction at point V.

Once calibrated, the model was then validated using data at the same tidal gauge stations but obtained from a different time period than that used for the calibration. In total five validation cases were tested and the RMSE values were calculated and averaged across all sixteen stations. Table 4 shows the results of the validation cases

Table 4. RMSE values for validation cases.

Case	Start Time	Average RMSE (m)
VAL1	01/03/2016 00:00	0.337
VAL2	01/04/2016 00:00	0.255
VAL3	01/05/2016 00:00	0.221
VAL4	01/06/2016 00:00	0.265
VAL5	01/07/2016 00:00	0.236

Validation cases 2-4 all have average RMSE values similar to the calibration case. Validation case 1 displayed a much larger difference in the RMSE value but can still be considered acceptable. The calibration and validation results show similar patterns to the obtained observed data suggesting that the 2D model is capable of accurately simulating the tidal conditions across the whole domain.

4 3D HYDRODYNAMIC MODELLING

The calibrated 2D model was further adapted to calculate the 3D hydrodynamics for the same domain. The model is composed of 10 layers which were sized at varying proportions of the water depth. The layers are more refined nearer the bed; with three layers in the top half of the depth and seven layers in the bottom half. These proportions were decided in order to accurately capture the variance in the near bed velocity. The 3D hydrodynamic model was run for a period of 30 days.

A cross-sectional profile consisting of 50 points with equal spacing of 1km was drawn over an area of the Indefatigable sandbanks in the north-west section of the domain for further analysis as shown in Figures 8 and 9.

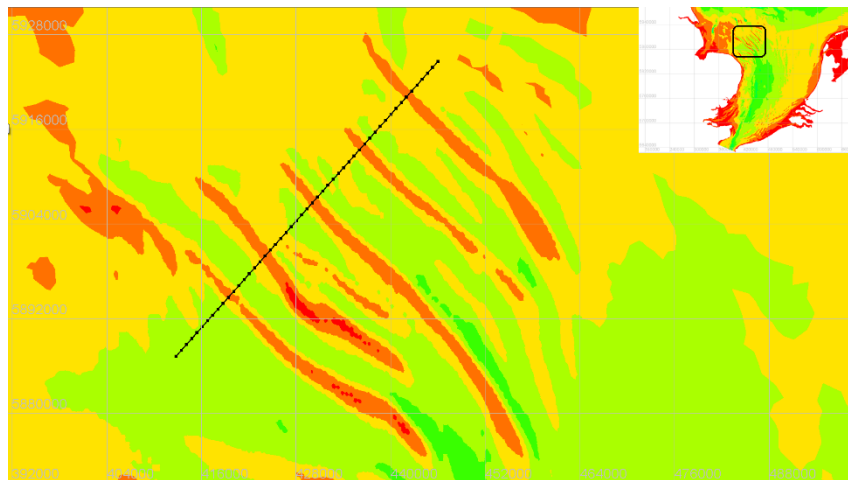


Figure 8. Location of the cross section within the computational domain.

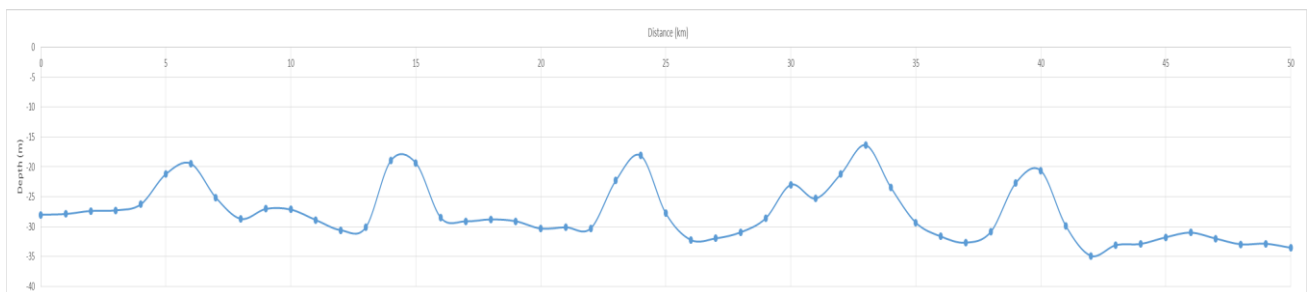


Figure 9. Bed elevation profile of the cross section

In order to determine the accuracy of the 3D model the depth averaged velocity was calculated from the velocity profiles by using the trapezium rule (shown in equation 3).

$$V = \sum \frac{1}{2} (v_l + v_{l+1}) (z_{l+1} - z_l) \quad [3]$$

Where;

- v_l is the velocity in layer l
- z is the depth ratio of layer l

The depth averaged flow of the 3D model was calculated at every timestep across each of the 50 points in the cross-section. Following this, the difference between the depth averaged velocity of the 3D model and the depth averaged velocity of the 2D model could be calculated. The average difference across all of the cross-sectional points and timesteps was found to be 0.0156ms^{-1} thus proving that the 3D model is still accurately representing the hydrodynamics of the region.

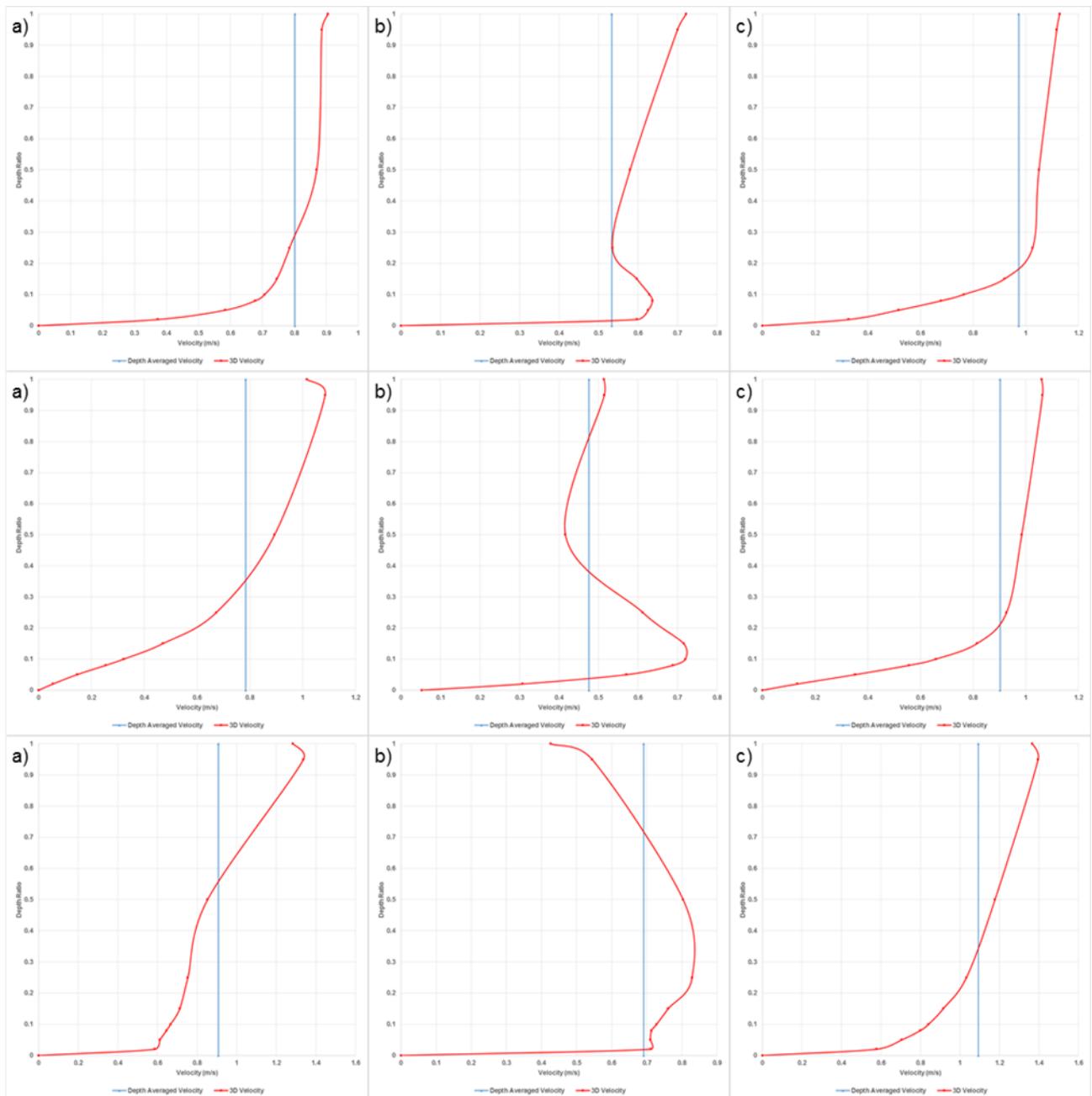


Figure 10. Velocity profiles during a) flood period b) high water and c) ebb period for points 23 (top), 25 (middle) and 28 (bottom) of the cross section.

Figure 10 shows the velocity profile at points 23, 25 and 28 representing the nearshore face, crest and offshore face of a sandbank respectively. At each point, a six hour period is covered; between 63-69 hours from the simulation start. It can be seen from the figures that during the flood and ebb periods, the maximum velocities occur near to the surface. At the high water level the maximum velocity occurs nearer to the bed. During the flood and ebb periods the near bed velocities are less than the depth averaged velocities.

Figure 11 shows the magnitude of the difference between the maximum velocity and the depth averaged velocity. Figure 11 shows that the differences tend to range between 0.2-0.4ms⁻¹ but can reach as high as 0.8ms⁻¹. The differences tend to be larger on the offshore face of the sandbank compared to the nearshore face and the crest. There is also a significant increase in the magnitude of the differences during spring tides compared to neap tides. The magnitude of the differences has implications for the estimations of sediment transport in the region. By only considering the depth averaged velocity, there is a tendency to overestimate the near bed sediment transport rates during the flood and ebb periods and underestimate them at the high water level. When considering the near surface velocities, the reverse is true. This means that erosion rates could be greater than previously anticipated which would cause more sediments to be transported offshore during high tide. Sediment eroded from the nearshore face of a sandbank may not necessarily be deposited on the offshore face due to the larger differences in velocity.

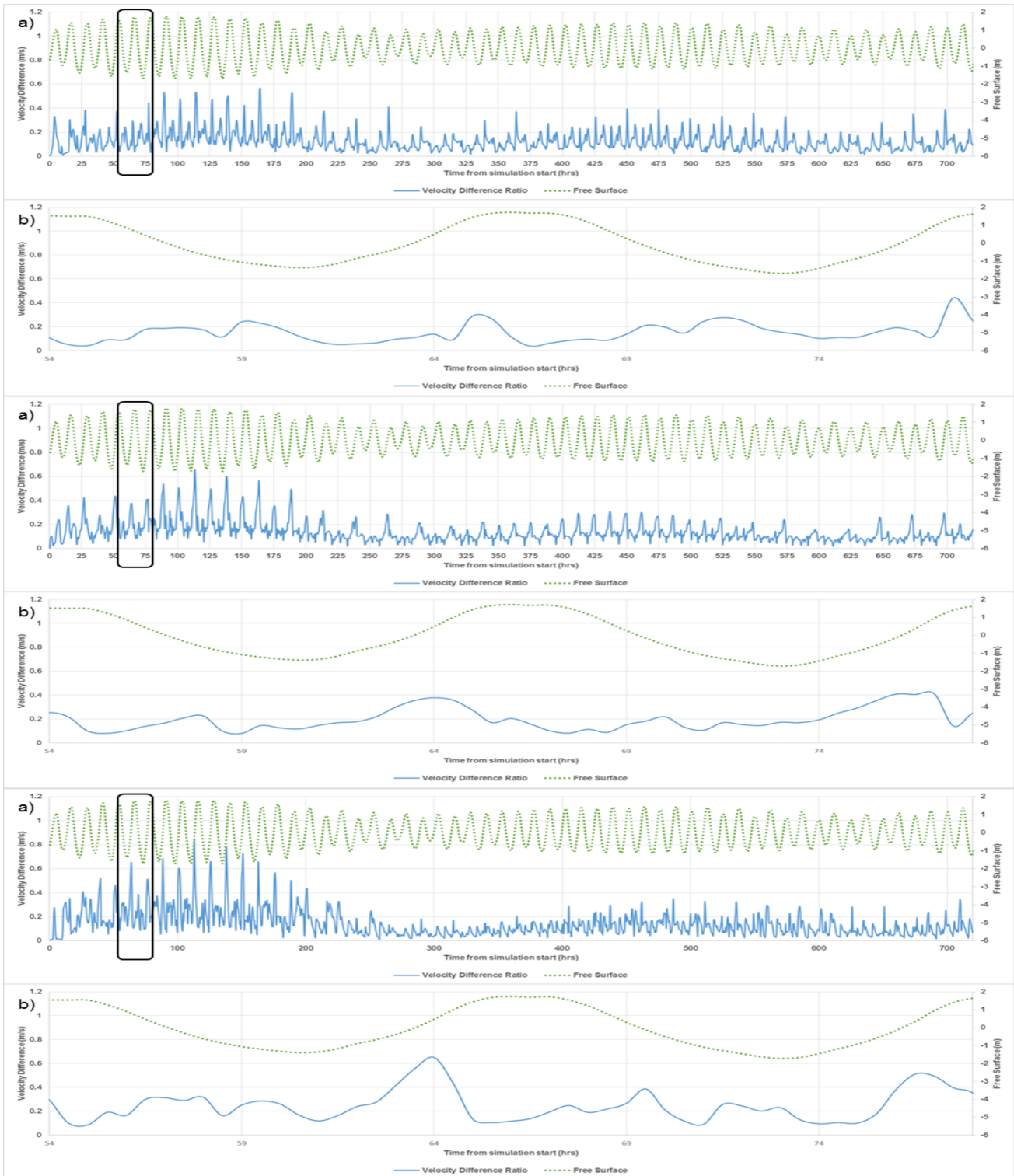


Figure 11. Difference between the maximum and depth averaged velocities for a) the whole simulation and b) a 24 hour period at points 23 (top), 25 (middle) and 28 (bottom).

5 CONCLUSIONS

This research aims to evaluate the differences between 2D and 3D hydrodynamic modelling on a study area in the North Sea. A 2D hydrodynamic model was set up using TELEMAC and then calibrated and validated against observation data obtained for the region. The calibration and validation processes were successful with RMSE values of 0.232m for the calibration cases and 0.221m for the validation cases. The model was then expanded to consider 3D hydrodynamics and analysis of the 3D velocity was completed along a cross section of the Indefatigable sandbanks. The analysis showed that there are large differences between the depth averaged velocity and the 3D velocity. The differences were higher during flood and ebb periods. Also the magnitude of the differences was much larger during spring tides compared to neap tides. This suggests that

the sediment transport rates would be underestimated when considering 2D velocity components and that erosion rates could be potentially higher than previously estimated.

ACKNOWLEDGEMENTS

This work was supported by the Engineering and Physical Sciences Research Council in the UK via grant EP/L016214/1 awarded for the Water Informatics: Science and Engineering (WISE) Centre for Doctoral Training, which is gratefully acknowledged.

This work uses data supplied by the BODC, REFMAR and the NOOS which is also gratefully acknowledged.

REFERENCES

- Besio, G., Blondeaux, P. & Vittori, G., 2005. A three-dimensional model of sand bank formation. *Ocean Dynamics*, 55(5), pp.515–525. Available at: <https://doi.org/10.1007/s10236-005-0027-0>.
- Brooks, S.M., 2010. *Coastal changes in historic times - linking offshore bathymetry changes and cliff recession in Suffolk*, London: The Crown Estate.
- Caston, V.N.D. & Stride, A.H., 1970. Tidal sand movement between some linear sand banks in the North Sea off northeast Norfolk. *Marine Geology*, 9(5), pp.M38–M42. Available at: <http://www.sciencedirect.com/science/article/pii/0025322770900186>.
- Chadwick, A., Fleming, C. & Reeve, D., 2012. *Coastal engineering : processes, theory and design practice*, London: London : Spon.
- Dyer, K.R. & Huntley, D.A., 1999. The origin, classification and modelling of sand banks and ridges. *Continental Shelf Research*, 19(10), pp.1285–1330. Available at: <http://www.sciencedirect.com/science/article/pii/S027843439900028X>.
- Garel, E., 2010. Tidally-averaged Currents and Bedload Transport over the Kwinte Bank, Southern North Sea. *Journal of Coastal Research*, Special Is(51), pp.87–94. Available at: <http://www.jstor.org/stable/40928821>.
- HR Wallingford, 2016. The TELEMAC-MASCARET modelling system. Available at: <http://www.opentelemac.org/index.php/presentation> [Accessed October 14, 2016].
- Jacoub, G. et al., 2007. Offshore sandbank morphodynamics modelling with sea level rise. Available at: http://ima.org.uk/_db/_documents/Jacoub.pdf.
- JNCC, 2017. Annex I Sandbanks in Offshore Waters. Available at: <http://jncc.defra.gov.uk/page-1452> [Accessed January 29, 2018].
- Kuang, C. & Stansby, P., 2006. Sandbanks for coastal protection: implications of sea-level rise. Part 2: current and morphological modelling. *Tyndall Centre Working Paper 87*.
- Oregon State University, 2010. The OSU TOPEX/Poseidon Global Inverse Solution - TPXO. Available at: <http://volkov.oce.orst.edu/tides/global.html> [Accessed May 16, 2018].
- Pan, S. et al., 2007. Modelling the hydrodynamics of offshore sandbanks. *Continental Shelf Research*, 27(9), pp.1264–1286. Available at: <http://www.sciencedirect.com/science/article/pii/S0278434307000337>.
- Stansby, P. et al., 2006. Sandbanks for coastal protection: implications of sea-level rise. Part 1: application to East Anglia. *Tyndall Centre Working Paper 86*.
- Stride, A.H., 1982. *Offshore tidal sands : processes and deposits*, London: Chapman and Hall.